Cubillos-Mesías et al. Radiation Oncology (2017) 12:190
DOI 10.1186/s13014-017-0931-8

Radiation Oncology

RESEARCH Open Access

Impact of robust treatment planning on single- and multi-field optimized plans for proton beam therapy of unilateral head and neck target volumes

Macarena Cubillos-Mesías[1*], Michael Baumann[1], Esther G. C. Troost[1,2,3,4,5], Fabian Lohaus[1,2,3], Steffen Löck[1,2,3], Christian Richter[1,2,3,4] and Kristin Stützer[1,4*]

Abstract

Background: Proton beam therapy is promising for the treatment of head and neck cancer (HNC), but it is sensitive to uncertainties in patient positioning and particle range. Studies have shown that the planning target volume (PTV) concept may not be sufficient to ensure robustness of the target coverage. A few planning studies have considered irradiation of unilateral HNC targets with protons, but they have only taken into account the dose on the nominal plan, without considering anatomy changes occurring during the treatment course.

Methods: Four pencil beam scanning (PBS) proton therapy plans were calculated for 8 HNC patients with unilateral target volumes: single-field (SFO) and multi-field optimized (MFO) plans, either using the PTV concept or clinical target volume (CTV)-based robust optimization. The dose was recalculated on computed tomography (CT) scans acquired during the treatment course. Doses to target volumes and organs at risk (OARs) were compared for the nominal plans, cumulative doses considering anatomical changes, and additional setup and range errors in each fraction. If required, the treatment plan was adapted, and the dose was compared with the non-adapted plan.

Results: All nominal plans fulfilled the clinical specifications for target coverage, but significantly higher doses on the ipsilateral parotid gland were found for both SFO approaches. MFO PTV-based plans had the lowest robustness against range and setup errors. During the treatment course, the influence of the anatomical variation on the dose has shown to be patient specific, mostly independent of the chosen planning approach. Nine plans in four patients required adaptation, which led to a significant improvement of the target coverage and a slight reduction in the OAR dose in comparison to the cumulative dose without adaptation.

Conclusions: The use of robust MFO optimization is recommended for ensuring plan robustness and reduced doses in the ipsilateral parotid gland. Anatomical changes occurring during the treatment course might degrade the target coverage and increase the dose in the OARs, independent of the chosen planning approach. For some patients, a plan adaptation may be required.

Keywords: Proton therapy, Single-field optimization, Multi-field optimization, Robust optimization, Adaptive radiation therapy, Head and neck cancer

* Correspondence: macarena.cubillos@oncoray.de; k.stuetzer@hzdr.de
[1]OncoRay – National Center for Radiation Research in Oncology, Faculty of Medicine and University Hospital Carl Gustav Carus, Technische Universität Dresden, Helmholtz-Zentrum Dresden – Rossendorf, Dresden, Germany
Full list of author information is available at the end of the article

BioMed Central

© The Author(s). 2017 **Open Access** This article is distributed under the terms of the Creative Commons Attribution 4.0 International License (http://creativecommons.org/licenses/by/4.0/), which permits unrestricted use, distribution, and reproduction in any medium, provided you give appropriate credit to the original author(s) and the source, provide a link to the Creative Commons license, and indicate if changes were made. The Creative Commons Public Domain Dedication waiver (http://creativecommons.org/publicdomain/zero/1.0/) applies to the data made available in this article, unless otherwise stated.

Background

Radiation therapy for head and neck cancer (HNC) is one of the pillars of treatment, being a definitive (possibly combined with chemotherapy) or adjuvant (after surgery, possibly combined with chemotherapy) treatment option. Due to the complexity of the target volumes and the surrounding organs at risk (OAR), the treatment planning process is particularly challenging. In general, radiation therapy is delivered using high-energy photons. However, nowadays particle beam therapy, in particular proton beam irradiation, is increasingly being introduced in clinical practice [1]. Intensity modulated proton therapy (IMPT) was shown to be promising for the treatment of HNC in terms of high dose conformity, with reduced dose to the normal tissue in comparison with photon therapy [2–5].

Due to the physical characteristics of dose deposition, protons are more sensitive to uncertainties than photons. These uncertainties can arise from changes in the patient anatomy throughout the treatment course, by e.g. tumor shrinkage, different cavity filling or weight loss, from daily variations in patient setup, from uncertainties in the proton range due to the conversion of computed tomography (CT) numbers to stopping power ratios [6, 7] and due to uncertainties in the beam delivery system. The optimization method of pencil beam scanning (PBS) proton therapy plans can be single-field (SFO) or multi-field optimization (MFO). In SFO, the spot positions and weights of each proton field are optimized individually, so the resultant dose distribution by each field is uniform over the target volume. In MFO, the spots from all the fields are optimized together, generating highly conformal dose distributions. Unlike SFO, the dose from individual MFO fields can be relatively inhomogeneous [8, 9].

Previous studies have shown that the conventional planning target volume (PTV) concept is not sufficient for providing robustness in target coverage in proton therapy [6, 10, 11], although SFO plans plus PTV margins could provide enough robustness [8]. Different optimization methods have been investigated to optimize plans which are robust against setup and range uncertainties [12–14], and some of them are already available in commercial treatment planning systems (TPS). Such robust plans are generated based on the clinical target volume (CTV) and take certain scenarios of setup errors and proton range uncertainties into account.

Unilateral HNC targets are an indication for proton beam therapy in our institution in case of re-irradiation or subtypes of salivary tumors, such as adenoidcystic carcinoma. Although unilateral HNC targets might not be as challenging as bilateral targets, the chosen beam direction and configuration, which is patient dependent, as well as different dose distribution and proximity to organs at risk, can influence the plan robustness and might indicate a different strategy for robust planning. For example, van der Voort et al. [15] have shown that unilateral cases seem to be intrinsically less robust than bilateral cases using a minimax worst-case scenario optimization. Different PBS proton planning studies can be found in literature for bilateral HNC targets, but only a few of them consider unilateral targets [16–18]. However, in these studies the authors have only taken the dose distribution on the initial planning CT into account without considering anatomical changes that may occur during the treatment course. The aim of this study was therefore to compare SFO and MFO PBS proton plans in combination with robust optimization for unilateral HNC targets in terms of, e.g. target coverage, dose reduction to the OARs, and to assess the robustness to range and setup uncertainties as well as to anatomical changes.

Methods

Patient data

Eight subsequent patients with unilateral head and neck tumors, treated with double scattering proton therapy at the University Proton Therapy Dresden were selected (Table 1). Each dataset consisted of a planning CT (pCT) and several control CTs (cCT) (median: 6, range: 3–13) acquired during the course of treatment using an in-room dual energy CT on-rails. For both, planning and cCTs, pseudo-monoenergetic CT data sets (79 keV) were reconstructed from dual-energy CT scans (80 kVp/140 kVp) [7].

CTVs and OARs spinal cord, brainstem, parotid gland, larynx, oral mucosa, pharyngeal constrictor muscles and esophageal inlet muscle were contoured on the pCT by an experienced radiation oncologist. A high-risk CTV including primary tumor, surgical cavity and potentially metastatic lymph nodes was expanded by the elective lymph nodes to generate a low-risk CTV. The pCT was registered with each cCT, the contours were transferred using a deformable registration algorithm [19], reviewed and if necessary corrected by the same radiation oncologist.

Treatment planning

The PTVs were generated for non-robust optimized plans by isotropic expansion of the CTVs by 5 mm to account for setup and range uncertainties [11]. The prescribed doses were 50.3 Gy(RBE) to the low-risk and 68 Gy(RBE) to the high-risk CTV, delivered by simultaneous integrated boost (SIB) in 34 fractions.

Four PBS proton plans were generated for each patient:

Table 1 Patient characteristics, volume of CTVs and details on imaging for verification

Patient	Primary tumor site	Gender	Clinical/ pathological TNM-stage	No. of cCTs	CTV / cm^3			
					Low-risk		High-risk	
1	Mucoepidermoid carcinoma of left parotid gland	F	pT1 N0 M0	6	159.7	(150.5–158.7)	17.1	(15.5–17.8)
2	Adenoidcystic carcinoma of right parotid gland	M	pT1 N0 M0	13	92.3	(87.7–96.3)	44.5	(42.3–46.4)
3	Small salivary glands of oral cavity	M	pT1 N2b M0	5	218.2	(199.9–211.2)	55.9	(50.3–53.3)
4	Lateral border of tongue	F	pT1 N2b M0	11	79.8	(79.0–83.9)	16.0	(16.2–17.1)
5	Right tonsil	M	pT2 N2b M0	11	150.2	(136.2–157.0)	43.2	(39.2–45.5)
6	Maxillary sinus	M	rcT2 N1 M0	5	134.9	(130.3–141.5)	28.8	(24.2–27.7)
7	Adenoidcystic carcinoma of left parotid gland	M	pT4a N0 M0	3	246.0	(238.4–242.6)	93.7	(87.9–91.7)
8	Recurrent adenoidcystic carcinoma of right submandibular gland	M	rpT2 N0 M0	6	78.7	(78.1–81.9)	22.5	(23.1–24.0)

Abbreviations: *F* Female, *M* Male, *cCT* Control CTs, *CTV* Clinical target volume
CTV values: pCT (range in cCTs)

- Conventional SFO and MFO plans with PTV concept, i.e. using the PTVs as target volumes (SFO_{PTV}, MFO_{PTV}).
- Robust optimized SFO and MFO plans (SFO_{Rob}, MFO_{Rob}), using the CTVs as target volumes and accounting 3 mm for setup uncertainty and 3.5% for range uncertainty, as used in our institution, considering in total 21 different scenarios in the minimax approach [6, 13]. Objective functions related to the target volumes were selected for robust optimization [20].

The plans were calculated and analyzed in RayStation v4.99 (RaySearch Laboratories AB, Stockholm, Sweden), considering a relative biological effectiveness (RBE) of 1.1. Two or three beams were used with the same configuration for the four different plans, avoiding entering through risk structures and inhomogeneity regions, with gantry angles between 15°-40° for the first beam, 70°-80° for the second beam and 160°-170° for the third beam, with couch rotations between 0°-20°. An IBA universal nozzle beam, with a pencil beam spot size sigma ranging from 8 mm (100 MeV) to 4 mm (220 MeV) was used for the calculations. The spot distance was calculated automatically by the TPS. Moreover, a calculation dose grid of 3x3x3 mm^3 and a range shifter of 7.5 cm water equivalent thickness were considered. An additional transitional intermediate volume between low-risk and high-risk region of 10 mm margin was created [15] for the SIB dose gradient.

The four plans were optimized to deliver the prescribed dose to the target volumes ($D_{98\%} \geq 95\%$ and $D_{2\%} \leq 107\%$ of the prescribed dose, where $D_{98\%}$ and $D_{2\%}$ are the minimum doses to 98% and 2% of the target volume, respectively), while sparing the clinical OARs following the institutional protocol: spinal cord: maximum dose (D_{max}) < 45 Gy, brainstem: D_{max} < 54 Gy and parotid gland: median dose (D_{median}) ≤ 26 Gy. The remaining OARs were considered for dose reporting.

Nominal plan robustness against setup and range uncertainty

For evaluating the plan robustness on the pCT, perturbed doses with random setup uncertainties and fixed range uncertainty values of −3.5%, 0% and 3.5% were generated. For each treatment fraction, a random number was drawn from a Gaussian distribution with mean μ = 0 mm and standard deviation σ = 2.5 mm [21, 22] for the isocenter shift in each cardinal direction (x, y, z). For each range uncertainty (−3.5% / 0% / 3.5%), 34 single-fraction doses with different random setup uncertainties were calculated on the pCT and summed to generate a new perturbed integral-treatment dose, which takes into account the random variation of the setup error in each fraction. This procedure was repeated 10 times for each range uncertainty scenario as displayed in Fig. 1, resulting in 30 cumulated perturbed doses considering only the anatomy from the pCT ($\overline{D}_{pCT}$). The dose-volume histograms (DVH) from the 30 results were plotted as DVH bands [23] for visual comparison.

Doses on control CTs

The four nominal plans per patient were recalculated in each cCT, in order to evaluate the influence of the anatomical changes on the dose distributions. For comparing the approximated delivered dose with the nominal plan, cumulative doses (D_{cCT}) were calculated by deforming [19] and summing the fraction doses from the cCTs on the pCT.

The plan robustness against setup and range errors including the anatomical changes was evaluated following the procedure as for the nominal plan. Again, 30 cumulative perturbed doses ($\overline{D}_{cCT}$) were generated, each with the same range error and 34 random setup errors, but

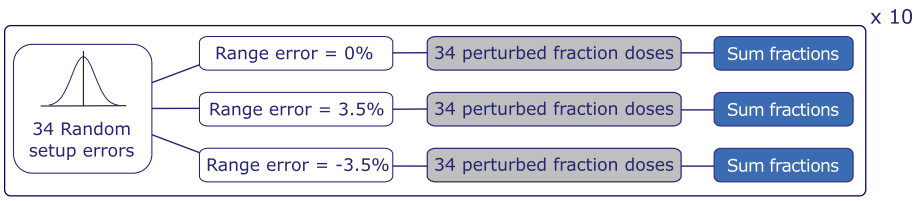

Fig. 1 Generation of 30 randomly perturbed dose distributions for the whole treatment course of 34 fractions

using the different cCTs for the respective fraction dose calculations.

Plan adaptation

An adaptive planning strategy was applied to compensate for anatomy-related discrepancies between nominal and fraction doses. Each fraction dose recalculated in the cCTs was compared with the nominal plan, considering the $D_{98\%}$ for low- and high-risk CTV and $D_{2\%}$ for high-risk CTV as dose parameters. Whenever a worsening of >5 percentage points between planned and unperturbed fraction dose was found [24], an adapted plan using the cCT of the respective fraction was calculated. Same beam configurations and objective functions as in the original plan were used.

A cumulative dose ($D_{\mathrm{cCT,\ Adapt}}$) was calculated as the sum of the fraction doses from the initial plan before adaptation plus the fraction doses with adapted plan. For practical purposes, the adaptation was considered to be initiated at the third fraction after the control CT with insufficient dose parameters to simulate a clinical scenario with required QA procedures for the new plan. This new adapted cumulative dose $D_{\mathrm{cCT,\ Adapt}}$ was compared with the cumulative doses without adaptation D_{cCT}.

Statistical analysis

One-way analysis of variance (ANOVA) followed by post-hoc two-sample independent *t*-tests were performed in SPSS (IBM Corporation, New York, USA) to find significant differences in dose parameters between the four nominal plans, including Bonferroni correction for multiple testing. Paired *t*-tests were used to determine significant differences between the planned dose D_{pCT}, the cumulative dose D_{cCT}, and the adapted cumulative dose $D_{\mathrm{cCT,\ Adapt}}$. Two-sided tests were performed and *p*-values <0.05 were considered to be significant.

Results

Evaluation of nominal plans

Dose distributions for an exemplary patient are shown in Fig. 2. For all patients, target coverage was similar for the four plans, fulfilling the specification ($D_{98\%}$: 96.9–100.5% for the low-risk CTV, 97.4–100.8% for the

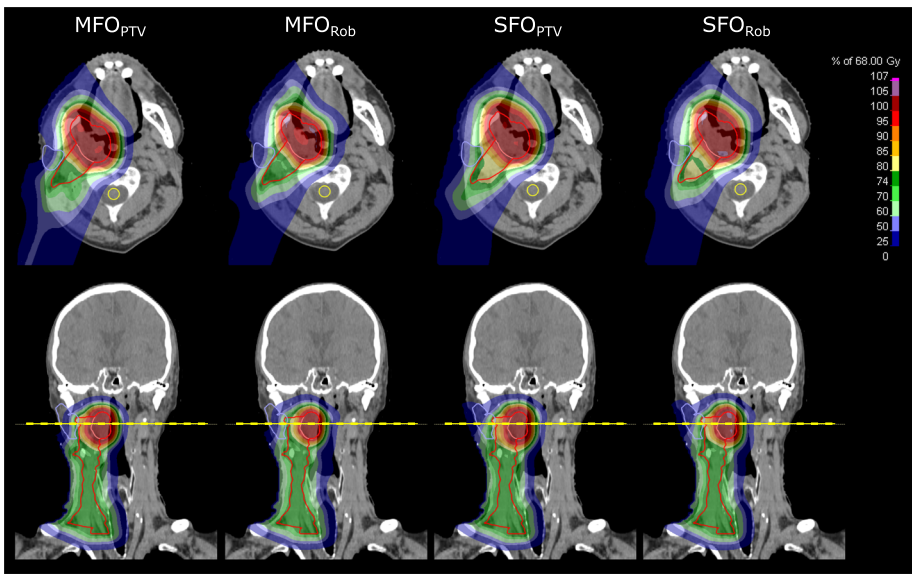

Fig. 2 Dose distributions for an example patient, in transversal (top) and coronal (bottom) view. The high-risk CTV is contoured in light red, the low-risk CTV in dark red, the ipsilateral parotid gland in light blue and the spinal cord (in the transversal view only) in yellow. The yellow dashed line indicates the location of the transversal view

high-risk CTV), but being slightly lower for the robust optimized plans, as displayed in Fig. 3. Regarding hot spots, $D_{2\%} \leq 107\%$ was met by the four plans in the high-risk CTV (103.6–106.3%). D_2 values higher than 107% can be found in the low-risk CTV due to the dose gradient for the SIB treatment, and were therefore not evaluated.

The doses to the OARs were similar for all planning strategies (Fig. 3). The near-maximum doses to the spinal cord (D_{1cc}: 0.36–12.05 Gy(RBE)) and brainstem (D_{1cc}: 0.01–6.17 Gy(RBE)) were far below the clinical constraints. For the ipsilateral parotid (only contoured in five patients due to surgical removal in the others), higher median doses were found in both SFO approaches. This dose increase was statistically significant for the SFO_{PTV} plans (ANOVA: $p = 0.005$; MFO_{PTV} vs. SFO_{PTV}: $p = 0.026$, MFO_{Rob} vs. SFO_{PTV}: $p = 0.006$). The contralateral parotid was completely spared in all cases (D_{median}: 0-0.1 Gy(RBE)). For the mean dose in the larynx, oral mucosa, constrictor muscles and esophageal inlet muscle, the doses between the four planning approaches were similar. Integral doses to the normal tissue [25] presented no differences between the different plans (mean values averaged over patient cohort: 36.47–37.84 Gy • Liter, standard deviation: 9.70–10.79 Gy • Liter). The 30 perturbed cumulated doses $\overline{D}_{pCT}$ resulted in wider DVH bands for the CTVs in the case of MFO_{PTV} plans, while the other 3 planning approaches showed a smaller and comparable band width (Fig. 4a). A high dose tail in the low-risk CTV can be observed in the PTV approaches, due to the PTV margin expansion used for both CTVs. An additional patient example can be found in Additional File 1: Fig. S1a, possessing wider DVH bands for both CTVs.

Evaluation of control CTs

The differences between the cumulative doses considering the anatomical variations in the control CTs (D_{cCT}) with the initial anatomy (D_{pCT}) are presented in Table 2. Comparing the differences $D_{cCT} - D_{pCT}$, high discrepancies on the target doses were observed for the MFO_{PTV} plan in one case, in which the hotspot dose in the high-risk CTV was increased by up to 5.5%.However, when analyzing the whole patient cohort, these variations were not statistically significant, compared to the other three plan approaches. The $D_{98\%}$ showed no significant differences in the low-risk CTV, whereas for the high-risk CTV the SFO_{Rob} plans revealed a significant $D_{98\%}$ reduction in the D_{cCT} of 0.78% ($p = 0.012$). Regarding the OARs, individual cases presented higher cumulative doses than the planned ones (e.g. up to 8 Gy in larynx D_{mean} for MFO_{PTV} and SFO_{PTV} plans in one patient). Table 3 shows target volume changes from the pCT to the last cCT. For some patients, volume shrinkage in both targets are observed (e.g. patient 3 and 5), whereas for other patients slight increase was found (e.g. patient 4 and 6).

When evaluating the robustness against setup and range errors while considering the anatomical changes ($\overline{D}_{cCT}$), again the MFO_{PTV} plans show wider bands in the CTV region as can be seen in Fig. 4b for the high-risk CTV. An additional patient example can be found in Additional File 1: Fig. S1b, possessing wider DVH bands for both CTVs.

Plan adaptation evaluation

Nine plans from 4 patients required plan adaptation, as summarized in Table 4. Four PTV-based plans and 5 robustly optimized plans needed adaptation.

Table 5 compares for the 9 adapted cases the differences between the nominal plan D_{pCT}, the cumulative dose D_{cCT} and the cumulative adapted dose $D_{cCT,\ Adapt}$. The target coverage in the cumulative dose was improved after adaptation ($p = 0.013$ for $D_{98\%}$(low-risk CTV), $p = 0.017$ for $D_{98\%}$(high-risk CTV)). The mean dose to the larynx was reduced in the adapted plans, whereas the other OARs showed no major

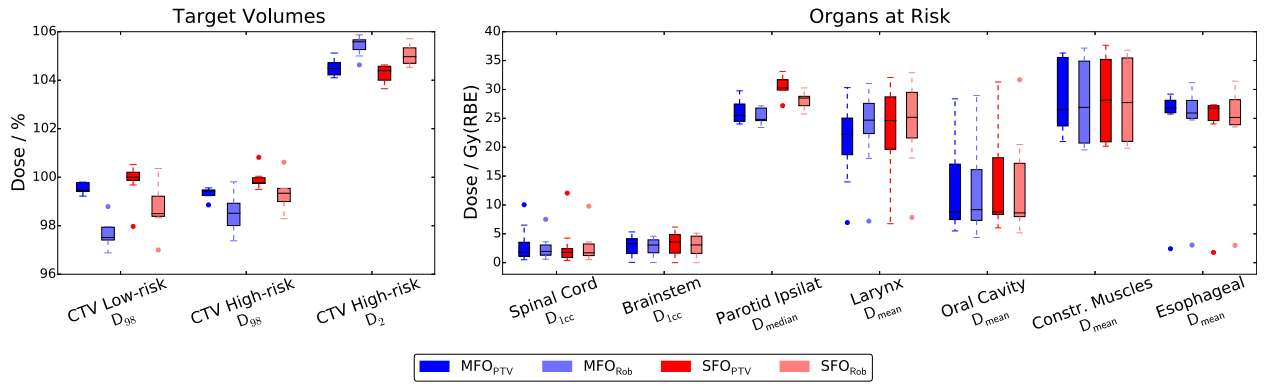

Fig. 3 Dose statistics from the 8 patients for target volumes (left) and organs at risk (right) in the nominal plans

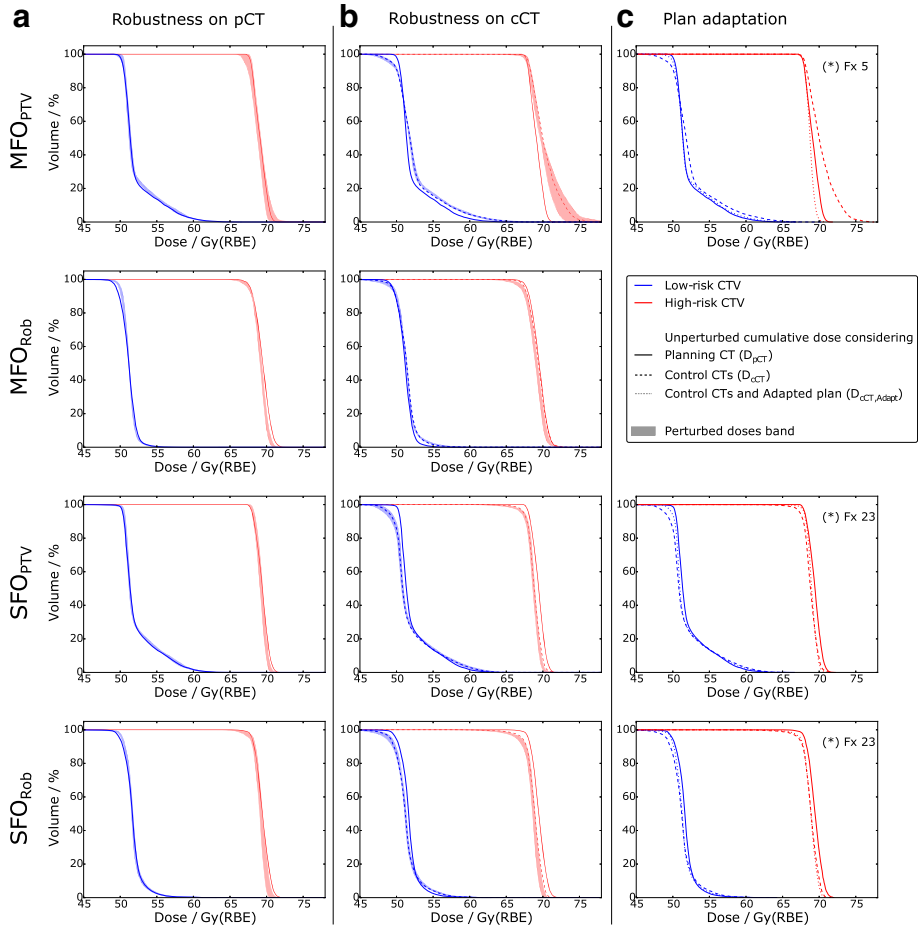

Fig. 4 DVHs from the four planning approaches MFO_{PTV}, MFO_{Rob}, SFO_{PTV} and SFO_{Rob} (top to bottom) for the low- (blue) and high-risk CTV (red) of an example patient who received plan adaptation for 3 plans after the 5th and 23th fraction. The DVH from the nominal plan (solid line, shown in all plots for orientation) is complemented by the DVH bands from the 30 perturbed cumulative doses for robustness analysis considering the initial plan and (**a**) the nominal anatomy ($\overline{D}_{pCT}$), and (**b**) anatomy in the control CTs ($\overline{D}_{cCT}$). DVH from the unperturbed cumulative dose considering the anatomical changes and additional plan adaptation (**c**) are indicated by dashed and dotted lines. (*) indicates the fraction number of the control CT when the adaptation demand was found

improvement, except in individual cases (e.g. mean dose of the esophageal inlet muscle reduced by 9.6 Gy for patient 3 in the adapted MFO_{PTV} plan). Fig. 4c includes DVHs of $D_{cCT,\ Adapt}$ for an example patient.

Discussion

We compared four different PBS proton therapy approaches for HNC patients with unilateral target volumes, SFO and MFO with and without robust optimization. Furthermore, we studied the influence of anatomical changes on the dose distributions, and applied plan adaptation when needed.

The PTV-based non-robust and the CTV-based robust approaches fulfilled the target coverage requirements in the nominal plan. The near maximum doses to spinal cord and brainstem were below the clinical constrains due to the unilateral target location, which allowed for an increased dose sparing compared to bilateral targets. However, both SFO plans gave significantly higher median doses to the ipsilateral parotid than the MFO approaches. This can be explained by the reduced degrees of freedom in the field modulation in comparison with MFO, an issue already investigated for bilateral HNC targets [8]. The contralateral parotid gland was completely spared due to the chosen beam configuration, which reduces the risk of severe xerostomia [26]. The plan optimization did not focus on dose to the larynx, oral mucosa, constrictor muscles and esophageal inlet, but dose values for these organs were similar for the different planning approaches and the DVH values were close to or below the recommended constraints for reducing the risk of larynx edema and dysphagia [27]. The 5 mm PTV margin expansion was chosen from our experience in photon therapy. We hesitated to reduce this

Table 2 Median (range) of differences between the cumulated dose considering the anatomy in the control CTs, D_{cCT}, and the nominal plan dose D_{pCT}. A positive number indicates a higher value of D_{cCT}. Significant differences (paired *t*-test, $p < 0.05$) are marked by*

ROI Parameter	MFO_{PTV}	MFO_{Rob}	SFO_{PTV}	SFO_{Rob}
Low-risk CTV				
$\Delta D_{98\%}$ / pp	−0.09	0.16	0	0.05
	(−3.62–0.58)	(−0.58–0.58)	(−4.14–0.76)	(−2.70–0.32)
High-risk CTV				
$\Delta D_{98\%}$ / pp	0.15	−0.53	−0.18	−0.78*
	(−1.03–1.94)	(−3.41–0.16)	(−2.50–0.16)	(−2.65 – −0.21)
$\Delta D_{2\%}$ / pp	0.18	−0.31*	−0.46*	−0.63*
	(−0.29–5.51)	(−0.88 – −0.06)	(−0.91 – −0.13)	(−0.94 – −0.34)
Spinal Cord				
ΔD_{1cc} / Gy	0.57	0.61	0.46	0.59*
	(−1.21–1.15)	(−0.82–1.04)	(−0.72–0.99)	(−0.80–1.22)
Brainstem				
ΔD_{1cc} / Gy	0.61	0.13	0.15	0.17
	(−0.82–1.04)	(−0.14–1.80)	(−0.24–1.14)	(−0.17–1.39)
Parotid Ipsilateral				
ΔD_{median} / Gy	0.66	0.04	−0.31	−0.34
	(−0.02–2.39)	(−1.66–1.78)	(−2.02–1.34)	(−2.66–1.34)
Larynx				
ΔD_{mean} / Gy	1.21	0.89	1.21	0.9
	(−1.37–8.58)	(−1.28–6.60)	(−1.51–8.86)	(−1.29–6.97)
Oral Mucosa				
ΔD_{mean} / Gy	−0.05	0.02	0.01	0.06
	(−0.48–1.79)	(−0.20–1.61)	(−0.72–1.72)	(−0.71–1.54)
Constrictor Muscles				
ΔD_{mean} / Gy	0.1	−0.11	0.05	0.05
	(−2.05–2.83)	(−2.09–2.35)	(−2.45–4.16)	(−2.24–2.91)
Esophageal inlet				
ΔD_{mean} / Gy	0.57	0.44	0.57	0.5
	(−1.67–7.84)	(−1.20–5.23)	(−1.64–8.15)	(−1.28–5.53)

Abbreviations: *pp.* Percentage points, $D_{98\%}$ Minimum dose to the 98% of the target volume, $D_{2\%}$ Minimum dose to the 2% of the target volume, D_{mean} Mean dose, D_{median} Median dose

margin for non-robust planning. If we would choose a smaller margin, the median doses in the ipsilateral parotid gland could be reduced. However, as already mentioned, due to the field modulation in SFO the parotid doses might still exceed the clinical objectives.

The MFO_{PTV} plans showed reduced robustness against uncertainties, while the other 3 approaches provided sufficient robustness on target coverage. Due to their characteristics in dose deposition, MFO_{PTV} plans are more sensitive to uncertainties in both patient setup and proton range than SFO_{PTV} and robustly optimized plans. Therefore they bear the risk to deliver a dose inferior to the prescribed one to the targets and OARs (see Additional File 2: Fig. S1). Beam direction and configuration might also influence the robustness of the plans. We chose two or three beams simulating a realistic clinical scenario. Some studies have found no significant differences in CTV coverage and plan robustness when the beam number is increased for bilateral HNC targets [28, 29].

When considering the anatomical changes during the treatment course, for individual cases, it was found that a lower dose than the planned dose might be delivered to the CTVs. These differences were independent of the planning approach, showing that both SFO and MFO techniques are sensitive to anatomical changes, being the same for PTV-based and robust approaches. The same conclusion can be drawn for the dose to the OARs,

Table 3 Difference in cm^3 between target volume in planning CT and last control CT. Positive (negative) values correspond to volume reduction (increase). Patients who underwent plan adaptation are marked by*

Patient	Volume change (cm^3)	
	Low-risk CTV	High-risk CTV
1	8.11	−0.03
2*	3.98	2.19
3*	18.25	5.54
4	−1.97	−0.94
5*	7.79	2.27
6*	−6.60	4.46
7	7.61	5.76
8	−3.23	−1.41

where the highest dose changes were found for PTV-based plans, especially for the larynx, constrictor muscles and esophagus inlet muscle. Furthermore, the target volume changes and the need of adaptation were patient dependent: patient 3 presented in both targets volume shrinkage, whereas for patient 6, which also underwent into adaptation, presented a slight increase of the low-risk CTV and a moderate shrinkage of the high-risk CTV. For a detailed conclusion, the size of the patient cohort is not sufficient. When considering a worst case scenario including anatomical changes (see Additional File 2: Fig. S2), the doses to the OARs could be highly increased, and the target coverage reduced as well, in comparison to a worst case scenario only considering setup and range uncertainties. The influence of anatomical changes could not be sufficiently estimated by the plan robustness evaluation in the planning CT, which explains why both PTV-based and robust-based plans underwent adaptation with a comparable frequency.

In 7 of the 9 cases with plan adaptation, the delivery of the adapted plan started within the last 10 fractions

Table 4 Overview of adapted plans, the respective adaptation criteria and the fraction number of the control CT in which the adaptation demand was found

Patient	Plan	Adaptation criteria	Fraction
2	MFO_{Rob}	$\Delta D_{98\%}$ (low-risk CTV)	24
	SFO_{Rob}	$\Delta D_{98\%}$ (low-risk CTV)	24
3	MFO_{PTV}	$\Delta D_{2\%}$ (high-risk CTV)	6
	SFO_{PTV}	$\Delta D_{98\%}$ (low-risk CTV)	23
	SFO_{Rob}	$\Delta D_{98\%}$ (low-risk CTV)	23
5	MFO_{PTV}	$\Delta D_{2\%}$ (high-risk CTV)	17
6	MFO_{Rob}	$\Delta D_{98\%}$ (high-risk CTV)	25
	SFO_{PTV}	$\Delta D_{98\%}$ (high-risk CTV)	25
	SFO_{Rob}	$\Delta D_{98\%}$ (high-risk CTV)	25

Table 5 Median (range) of the dosimetric difference between the estimated delivered dose by the nominal (D_{pCT}), the cumulative (D_{cCT}) and adapted plan ($D_{cCT,\ Adapt}$) for the investigated 9 cases. A positive number indicates a higher value for D_{cCT}. Significant differences (paired *t*-test, $p < 0.05$) are marked by *

ROI Parameter	$D_{cCT} - D_{pCT}$	$D_{cCT} - D_{cCT,\ Adapt}$
CTV Low-risk		
$\Delta D_{98\%}$ / pp	−0.76*	−0.52*
	(−4.14–0.42)	(−2.76 – −0.14)
CTV High-risk		
$\Delta D_{98\%}$ / pp	−1.15*	−0.6*
	(−3.41–0.25)	(−2.22–0.25)
$\Delta D_{2\%}$ / pp	−0.34	0.37
	(−0.94–5.51)	(−0.13–6.74)
Spinal Cord		
ΔD_{1cc} / Gy	0.43	−0.15
	(−0.82–1.14)	(−0.22–0.79)
Brainstem		
ΔD_{1cc} / Gy	0.74*	0.22
	(−0.24–1.8)	(−0.19–1.07)
Parotid Ipsilateral		
ΔD_{median} / Gy	0	−0.26
	(−2.66–1.78)	(−1.16–0.73)
Larynx		
ΔD_{mean} / Gy	6.39*	1.69*
	(−1.51–8.86)	(−0.87–9.05)
Oral Mucosa		
ΔD_{mean} / Gy	−0.2	−0.23
	(−0.72–1.79)	(−0.66–2.29)
Constrictor Muscles		
ΔD_{mean} / Gy	0.66	0.22
	(−2.45–4.16)	(−0.86–4.26)
Esophagus		
ΔD_{mean} / Gy	0	0.13
	(−1.64–8.15)	(−0.93–9.61)

Abbreviations: *pp.* Percentage points, $D_{98\%}$ Minimum dose to the 98% of the target volume, $D_{2\%}$ Minimum dose to the 2% of the target volume, D_{mean} Mean dose, D_{median} Median dose

of the treatment. The adaptation was necessary due to an underdosage in the low- or high-risk CTV, except for two MFO_{PTV} plans, where the criterion was an overdose in the CTV high-risk. The cumulated dose from the adapted plans $D_{cCT,\ Adapt}$ improved the target coverage, but they did not improve the OAR dose in comparison to the cumulative doses without adaptation D_{cCT}, except for the larynx. The quite small, but partially significant improvements can be found because in most cases the number of fractions with adapted plan

was small, but the cumulative doses for the whole treatment were considered for the analysis. For bilateral HNC targets, Kurz et al. [30] did not find a significant difference in the target coverage between the recalculated dose in the control CT and the adapted plan, but the adaptation showed a reduction of overdosage ($D_{2\%}$) in the target volume. However, Góra et al. [31] found a large improvement in the target coverage with the generation of adapted MFO_{PTV} plans on a biweekly basis, whereas the OAR dose limits were not exceeded, even without adaptation. The difference between both studies might be explained because Kurz et al. optimized their adapted plan in a cone-beam CT (CBCT)-based virtual CT. It is known that proton dose calculations on CBCT-based images have limitations in accuracy due to several reasons [32, 33]. Hence, the CBCT-based adaptation might therefore not be as optimal as an adaptation planned directly on a control CT, as done by Góra et al. Besides, a strong case-dependency in bilateral HNC targets could be responsible for non-consistent results in the literature. In this work, the adaptation procedure was applied when a difference of >5 percentage points between planned and a single fraction dose was found. Probably in some cases the adaptation might also be necessary if many consecutive fractions show inferior target coverage, although each difference with the planned dose remains lower than 5 percentage points. Adaptation criteria considering the deviations of the tracked accumulated dose from the planned dose may be able to detect a reduction in the target coverage earlier than comparing it with the individual fraction doses. In the present study, only dose deviations in the target volumes were considered, but variations in the OARs dose parameters during the treatment course should be taken into account as well.

All the evaluations including calculation of SFO and MFO plans in combination with robust optimization, dose calculation in additional CTs, dose deformation and dose accumulation were performed in a commercial TPS, which means that the evaluation tools could be easily translated into clinical routine.

Conclusions

The four PBS planning approaches showed adequate target coverage on the nominal plan for unilateral HNC. For ensuring plan robustness and reduced median doses in the ipsilateral parotid gland, MFO_{Rob} is recommended. Both PTV-based and robust optimized plans were sensitive to anatomical changes for individual cases, leading to inferior target coverage and higher OARs dose, and requiring plan adaptation. None of the 4 planning approaches presented a clear superiority concerning the need of plan adaptation.

Additional files

Additional file 1: Dose-volume histograms for additional patient example. (PDF 156 kb)

Additional file 2: Worst case analysis. (PDF 423 kb)

Abbreviations

$D_{cCT,\ \underline{Adapt}}$: Cumulative adapted dose; $D_{\underline{cCT}}$: Cumulative dose; D_{pCT}: Nominal dose; $\overline{D_{cCT}}$: Perturbed cumulative dose; $\overline{D_{pCT}}$: Perturbed dose on the pCT; ANOVA: Analysis of variance; CBCT: Cone-beam CT; cCT: Control CT; CT: Computer tomography; CTV: clinical target volume; $D_{2\%}$: Minimum dose to the 2% of the target volume; $D_{98\%}$: Minimum dose to the 98% of the target volume; D_{mean}: Mean dose; D_{median}: Median dose; DVH: Dose-volume histogram; HNC: Head and neck cancer; IMPT: Intensity modulated proton therapy; MFO: Multi-field optimization; MFO_{PTV}: MFO PTV-based plan; MFO_{Rob}: MFO robust-optimized plan; OAR: Organ at risk; PBS: Pencil beam scanning; pCT: Planning CT; pp: Percentage points; PTV: Planning target volume; RBE: Relative biological effectiveness; ROI: Region of interest; SFO: Single-field optimization; SFO_{PTV}: SFO PTV-based plan; SFO_{Rob}: SFO robust-optimized plan; SIB: Simultaneous integrated boost; TPS: Treatment planning system

Acknowledgements

Not applicable.

Funding

This work was supported by the German Academic Exchange Service (DAAD – 57,129,429), the German Research Foundation (DFG – STU 668/1–1) and the German Federal Ministry of Education and Research (BMBF – 03Z1N51).

Availability of data and materials

The datasets generated and analyzed during the current study are not publicly available due to patient data protection, but are available from the corresponding author on reasonable request.

Authors' contributions

MCM performed treatment planning, data analysis, generated figures and was a major contributor in writing the manuscript. MB designed tools for robustness analysis which can be used in the TPS interface. ET participated in the study design, performed the delineation in planning and control CTs, approved the plans and edited the manuscript. FL performed the delineation in planning and control CTs. SL contributed with the statistical analysis of the data. CR participated in the study design, and edited the manuscript. KS participated in the study design, contributed in writing and editing the manuscript. All authors read and approved the final manuscript.

Ethics approval and consent to participate

The study was approved by the institutional Ethics Committee under the number EK 172042015.

Consent for publication

The patients gave their informed consent for use of the data for research purposes.

Competing interests

The authors declare that they have no competing interests.

Publisher's Note

Springer Nature remains neutral with regard to jurisdictional claims in published maps and institutional affiliations.

Author details

[1]OncoRay – National Center for Radiation Research in Oncology, Faculty of Medicine and University Hospital Carl Gustav Carus, Technische Universität Dresden, Helmholtz-Zentrum Dresden – Rossendorf, Dresden, Germany. [2]Department of Radiotherapy and Radiation Oncology, Faculty of Medicine and University Hospital Carl Gustav Carus, Technische Universität Dresden, Dresden, Germany. [3]German Cancer Consortium (DKTK), partner site Dresden, and German Cancer Research Center (DKFZ), Heidelberg, Germany.

[4]Helmholtz-Zentrum Dresden - Rossendorf, Institute of Radiooncology – OncoRay, Dresden, Germany. [5]National Center for Tumor Diseases (NCT), partner site Dresden, Dresden, Germany.

Received: 1 June 2017 Accepted: 22 November 2017
Published online: 28 November 2017

References

1. Baumann M, Krause M, Overgaard J, Debus J, Bentzen SM, Daartz J, et al. Radiation oncology in the era of precision medicine. Nat Publ Gr. 2016:8–11. https://doi.org/10.1038/nrc.2016.18.
2. Cozzi L, Fogliata A, Lomax A, Bolsi A. A treatment planning comparison of 3D conformal therapy, intensity modulated photon therapy and proton therapy for treatment of advanced head and neck tumours. Radiother Oncol. 2001;61:287–97. https://doi.org/10.1016/S0167-8140(01)00403-0.
3. Steneker M, Lomax A, Schneider U. Intensity modulated photon and proton therapy for the treatment of head and neck tumors. Radiother Oncol. 2006; 80:263–7. https://doi.org/10.1016/j.radonc.2006.07.025.
4. van de Water TA, Lomax AJ, Bijl HP, de Jong ME, Schilstra C, Hug EB, et al. Potential benefits of scanned intensity-modulated proton therapy versus advanced photon therapy with regard to sparing of the salivary glands in Oropharyngeal cancer. Int J Radiat Oncol. 2011;79:1216–24. https://doi.org/10.1016/j.ijrobp.2010.05.012.
5. Jakobi A, Bandurska-Luque A, Stützer K, Haase R, Löck S, Wack L-J, et al. Identification of patient benefit from proton therapy for advanced head and neck cancer patients based on individual and subgroup NTCP analysis. Int J Radiat Oncol Biol Phys. 2015;92:1165–74. https://doi.org/10.1016/j.ijrobp.2015.04.031.
6. Liu W, Frank SJ, Li X, Li Y, Park PC, Dong L, et al. Effectiveness of robust optimization in intensity-modulated proton therapy planning for head and neck cancers. Med Phys. 2013;40:51711. https://doi.org/10.1118/1.4801899.
7. Wohlfahrt P, Möhler C, Hietschold V, Menkel S, Greilich S, Krause M, et al. Clinical implementation of dual-energy CT for proton treatment planning on pseudo-monoenergetic CT scans. Int J Radiat Oncol Biol Phys. 2017;97: 427–34. https://doi.org/10.1016/j.ijrobp.2016.10.022.
8. Quan EM, Liu W, Wu R, Li Y, Frank SJ, Zhang X, et al. Preliminary evaluation of multifield and single-field optimization for the treatment planning of spot-scanning proton therapy of head and neck cancer. Med Phys. 2013;40: 81709. https://doi.org/10.1118/1.4813900.
9. Paganetti H. Proton therapy physics - series in medical physics and biomedical engineering. Illustrate. Boca Raton: CRC Press; 2011.
10. Liu W, Frank SJ, Li X, Li Y, Zhu RX, Mohan R. PTV-based IMPT optimization incorporating planning risk volumes vs robust optimization. Med Phys. 2013; 40:21709. https://doi.org/10.1118/1.4774363.
11. van Dijk LV, Steenbakkers RJHM, ten Haken B, van der Laan HP, van' t Veld AA, Langendijk JA, et al. Robust intensity modulated proton therapy (IMPT) increases estimated clinical benefit in head and neck cancer patients. PLoS One. 2016;11:e0152477. https://doi.org/10.1371/journal.pone.0152477.
12. Unkelbach J, Bortfeld T, Martin BC, Soukup M. Reducing the sensitivity of IMPT treatment plans to setup errors and range uncertainties via probabilistic treatment planning. Med Phys. 2009;36:149. https://doi.org/10.1118/1.3021139.
13. Fredriksson A, Forsgren A, Hårdemark B. Minimax optimization for handling range and setup uncertainties in proton therapy. Med Phys. 2011;38:1672. https://doi.org/10.1118/1.3556559.
14. Liu W, Zhang X, Li Y, Mohan R. Robust optimization of intensity modulated proton therapy. Med Phys. 2012;39:1079–91. https://doi.org/10.1118/1.3679340.
15. van der Voort S, van de Water S, Perkó Z, Heijmen B, Lathouwers D, Hoogeman M. Robustness recipes for minimax robust optimization in intensity-modulated proton therapy for oropharyngeal cancer patients. Int J Radiat Oncol Biol Phys. 2016;95 https://doi.org/10.1016/j.ijrobp.2016.02.035.
16. Kandula S, Zhu X, Garden AS, Gillin M, Rosenthal DI, Ang K-K, et al. Spot-scanning beam proton therapy vs intensity-modulated radiation therapy for ipsilateral head and neck malignancies: a treatment planning comparison. Med Dosim. 2013;38:1–5. https://doi.org/10.1016/j.meddos.2013.05.001.
17. Stromberger C, Cozzi L, Budach V, Fogliata A, Ghadjar P, Wlodarczyk W, et al. Unilateral and bilateral neck SIB for head and neck cancer patients. Strahlenther und Onkol. 2016;192:232–9. https://doi.org/10.1007/s00066-016-0945-4.
18. Romesser PB, Cahlon O, Scher E, Zhou Y, Berry SL, Rybkin A, et al. Proton beam radiation therapy results in significantly reduced toxicity compared with intensity-modulated radiation therapy for head and neck tumors that require ipsilateral radiation. Radiother Oncol. 2016;118:286–92. https://doi.org/10.1016/j.radonc.2015.12.008.
19. Weistrand O, Svensson S. The ANACONDA algorithm for deformable image registration in radiotherapy. Med Phys. 2014;42:40–53. https://doi.org/10.1118/1.4894702.
20. Li Y, Niemela P, Liao L, Jiang S, Li H, Poenisch F, et al. Selective robust optimization: a new intensity-modulated proton therapy optimization strategy. Med Phys. 2015;42:4840–7. https://doi.org/10.1118/1.4923171.
21. van Kranen S, van Beek S, Rasch C, van Herk M, Sonke JJ. Setup uncertainties of anatomical sub-regions in head-and-neck cancer patients after offline CBCT guidance. Int J Radiat Oncol Biol Phys. 2009;73:1566–73.
22. Velec M, Waldron JN, O'Sullivan B, Bayley A, Cummings B, Kim JJ, et al. Cone-beam CT assessment of Interfraction and Intrafraction setup error of two head-and-neck cancer thermoplastic masks. Int J Radiat Oncol Biol Phys. 2010;76:949–55.
23. Trofimov A, Unkelbach J, Delaney TF, Bortfeld T. Visualization of a variety of possible dosimetric outcomes in radiation therapy using dose-volume histogram bands. Pract Radiat Oncol. 2012;2:164–71. https://doi.org/10.1016/j.prro.2011.08.001.
24. Placidi L, Bolsi A, Lomax AJ, Schneider RA, Malyapa R, Weber DC, et al. The effect of anatomical changes on pencil beam scanned proton dose distributions for cranial and extra cranial tumors. Int J Radiat Oncol Biol Phys. 2016; https://doi.org/10.1016/j.ijrobp.2016.11.013.
25. Yang R, Xu S, Jiang W, Xie C, Wang J. Integral dose in three-dimensional conformal radiotherapy, intensity-modulated radiotherapy and helical tomotherapy. Clin Oncol (R Coll Radiol). 2009;21:706–12. https://doi.org/10.1016/j.clon.2009.08.002.
26. Deasy JO, Moiseenko V, Marks L, Chao KSC, Nam J, Eisbruch A. Radiotherapy dose–volume effects on salivary gland function. Int J Radiat Oncol Biol Phys. 2010;76:S58–63. https://doi.org/10.1016/j.ijrobp.2009.06.090.
27. Rancati T, Schwarz M, Allen AM, Feng F, Popovtzer A, Mittal B, et al. Radiation dose–volume effects in the larynx and pharynx. Int J Radiat Oncol. 2010;76:S64–9. https://doi.org/10.1016/j.ijrobp.2009.03.079.
28. Kraan AC, Van De Water S, Teguh DN, Al-Mamgani A, Madden T, Kooy HM, et al. Dose uncertainties in IMPT for oropharyngeal cancer in the presence of anatomical, range, and setup errors. Int J Radiat Oncol Biol Phys. 2013;87: 888–96. https://doi.org/10.1016/j.ijrobp.2013.09.014.
29. Barten DLJ, Tol JP, Dahele M, Slotman BJ, Verbakel WFAR. Comparison of organ-at-risk sparing and plan robustness for spot-scanning proton therapy and volumetric modulated arc photon therapy in head-and-neck cancer. Med Phys. 2015;42:6589–98. https://doi.org/10.1118/1.4933245.
30. Kurz C, Nijhuis R, Reiner M, Ganswindt U, Thieke C, Belka C, et al. Feasibility of automated proton therapy plan adaptation for head and neck tumors using cone beam CT images. Radiat Oncol. 2016;11:64. https://doi.org/10.1186/s13014-016-0641-7.
31. Góra J, Kuess P, Stock M, Andrzejewski P, Knäusl B, Paskeviciute B, et al. ART for head and neck patients: on the difference between VMAT and IMPT. Acta Oncol. 2015:1–9. https://doi.org/10.3109/0284186X.2015.1028590.
32. Veiga C, Janssens G, Teng C-L, Baudier T, Hotoiu L, McClelland JR, et al. First clinical investigation of cone beam computed tomography and deformable registration for adaptive proton therapy for lung cancer. Int J Radiat Oncol. 2016;95:549–59. https://doi.org/10.1016/j.ijrobp.2016.01.055.
33. Kurz C, Kamp F, Park Y-K, Zöllner C, Rit S, Hansen D, et al. Investigating deformable image registration and scatter correction for CBCT-based dose calculation in adaptive IMPT. Med Phys. 2016;43:5635–46. https://doi.org/10.1118/1.4962933.